View metadata, citation and similar papers at core.ac.uk
brought to you by CORE

学位論文

「Roles of Receptor Activity-Modifying Protein 1 in Angiogenesis and Lymphangiogenesis during Skin Wound Healing in Mice」

（マウス創傷治癒時の血管新生・リンパ管新生における

受容体活性調節蛋白１の役割）

ＤＭ１００１５　藏重　千絵

北里大学大学院医療系研究科医学専攻博士課程
臨床医科学群　麻酔科学
指導教授　岡本　浩嗣

著者の宣言

本学位論文は、著者の責任において実験を遂行し、得られた真実の結果に基づいて正確に作成したものに相違ないことをここに宣言する。

要旨

【背景】受容体活性調節蛋白１（RAMP1）は、カルシトニン受容体様受容体（CLR）とヘテロダイマーを形成し、カルシトニン遺伝子関連ペプチド（CGRP）受容体を形成している。CGRP は 37 個のアミノ酸からなるポリペプチドであり、主に神経系に幅広く発現し、多様な生理作用が知られている。分子薬理研究室では、これまでにさまざまなモデルを用いて CGRP が血管新生に関与しているということを報告してきた。本研究では RAMP1 に着目し、創傷の治癒過程および創傷部位の脈管新生における CGRP-RAMP1 シグナルの役割について検討を行った。

【方法】8 週齢の野生型 C57BL/6 雄性マウス（WT）および RAMP1-/-を使用し、創傷治癒モデルを作成した。マウス背部の皮膚に直径 6mm の創を作成し、WT と RAMP1-/-とで治癒経過を比較した。また創傷肉芽組織を対象として、免疫組織化学的評価や real time PCR を行い、脈管新生の評価を行った。

【結果および考察】WT に比べ RAMP1-/-では、早期における創傷治癒の遅延が認められた。また、肉芽組織における血管内皮マーカーCD31 の免疫染色では、RAMP1-/-で血管密度が有意に抑制された。また real-time PCR を行い、肉芽組織における CD31 と血管新生増強因子 VEGF-A の発現量を調べたところ、いずれも治癒早期の段階で RAMP1-/-において発現の抑制が認められた。これらの結果から、創傷部の肉芽組織における VEGF-A を介した血管新生に CGRP-RAMP1 シグナルが関与していることが示唆された。

次に、抗 RAMP1 抗体および抗 CD31 抗体を用いて免疫染色を行い、血管における RAMP1 の局在について評価したところ、創周辺部の健常皮膚組織の血管上には RAMP1 の発現が認められたが、肉芽組織内の新生血管上には RAMP1 の発現が認められなかった。この結果から、CGRP-RAMP1 シグナルは血管新生には関与するものの、新生血管の内皮細胞には直接的に作用していない可能性が考えられた。

そこで、肉芽の主要構成細胞である線維芽細胞とマクロファージに着目し、それぞれの細胞上に RAMP1 が発現しているか検討を行った。繊維芽細胞に対しては抗 S100A4 抗体、マクロファージに対しては抗 CD11b 抗体を用いて、抗 RAMP1 抗体との二重染色を行ったところ、それぞれ共発現部位が観察されたことから、線維芽細胞とマクロファージの表面に RAMP1 が発現していることが分かった。

そこで次に in vitro の検討として、線維芽細胞とマクロファージを CGRP アゴニストで刺激し、VEGF-A の遺伝子発現量の変化を評価した。その結果、繊維芽細胞の細胞株である L929 では VEGF-A の発現は減少したが、マクロファージでは VEGF-A の発現が用量依存的に増加した。この結果から、マクロファージ上の RAMP1 が CGRP の刺激を受けて、VEGF-A の産生を促進し、血管新生を誘導し

ていることが示唆された。
また同実験において、リンパ管新生増強因子 VEGF-C および VEGF-D の遺伝子発現量の変化についても評価した。その結果、L929 では VEGF-C・VEGF-D いずれも発現量に変化は認められなかった。一方マクロファージでは、VEGF-D の発現量に変化は認められなかったが、VEGF-C の発現は用量依存的に増加した。この結果から、マクロファージが CGRP の刺激を受けて、VEGF-C の産生を促進し、リンパ管新生も誘導している可能性が考えられた。

そこで、肉芽組織におけるリンパ管内皮マーカーLYVE-1 の免疫染色を行い、リンパ管新生を評価してみると、RAMP1-/-でリンパ管密度が有意に抑制された。また real-time PCR を行い、肉芽組織における VEGF-C とリンパ管内皮マーカーVEGFR-3 の発現量を調べたところ、いずれも治癒早期から中期にかけて RAMP1-/-において発現の抑制が認められた。さらに、創作成後 7 日目のマウスの創直下に FITC デキストランを投与し、新生リンパ管のドレナージ機能を評価したところ、RAMP1-/-ではリンパ管新生の抑制に伴いドレナージ機能が有意に抑制された。これらの結果から、創傷部の肉芽組織における VEGF-C を介したリンパ管新生に CGRP-RAMP1 シグナルが関与していることが示唆された。

次に、創傷肉芽組織のマクロファージは骨髄から動員されてくることが知られているため、骨髄移植モデルを作成し、骨髄由来マクロファージが創傷部へ動員され治癒を促進しうるかどうか、また動員された際の CGRP-RAMP1 シグナルの役割について検討を行った。
WT の骨髄を移植したマウスと RAMP1-/-の骨髄を移植したマウスとで創傷治癒経過を比較すると、RAMP1-/-骨髄移植マウスでは、早期における創傷治癒の遅延が認められた。
また肉芽組織の免疫染色では、RAMP1-/-骨髄移植マウスにおいて血管密度・リンパ管密度が有意に抑制された。これらの結果から、創傷治癒時の肉芽組織では、骨髄から動員されたマクロファージが CGRP の刺激を受け、VEGF-A、VEGF-C の産生を介して血管新生・リンパ管新生を増強させることが明らかとなった。

【結論】今回の実験から、創傷治癒過程における脈管新生には、CGRP-RAMP1 シグナル伝達による VEGF 誘導の重要性が示唆された。RAMP1 は血管新生やリンパ管新生がかかわる疾患の治療標的として重要であると考えられる。

Contents

1. Introduction

Calcitonin gene-related peptide (CGRP) is a 37-aa neuropeptide that is produced in the neural body of dorsal root ganglion (DRG) cells and released from sensory nerve endings. Receptor activity-modifying proteins (RAMPs) are a family of proteins that interact with and modulate the activities of several class B G-protein-coupled receptors (GPCRs). The RAMP protein family consists of 3 members, RAMP1, RAMP2, and RAMP3, each of which is encoded by a separate gene and has diverse spatiotemporal expression patterns (1). CGRP binds to CGRP receptors composed of RAMP1 and calcitonin receptor-like receptor (CLR) to modulate various functions, such as vasodilation and pain transmission (2, 3). CGRP couples to the activation of adenylate cyclase (AC) to elevate cAMP levels; however, biochemical and pharmacologic studies in cultured cells show that RAMPs can modulate additional aspects of CGRP receptor signaling, including receptor trafficking, ligand binding affinity, second-messenger signaling and receptor desensitization. Several gene-targeted knockout and transgenic models have been generated and characterized in recent years (4).

CLR is a common receptor subunit for both CGRP and adrenomedullin (AM), a 52-aa peptide that shares some degree of homology with CGRP (5). The specificity of the CGRP receptor is believed to be decided by RAMP1, in light of the finding that the N terminus of RAMP1 is essential for CGRP binding (6). To elucidate the physiological functions of CGRP mediated through CLR/RAMP1 receptors in vivo, we generated RAMP1-deficient (RAMP1-/-) mice by using a conditional gene-targeting technique. We discovered that these mice exhibit potent hypertension, but their heart rate is unaffected (7). In addition, the RAMP1-/- mice exhibit a significant increase in serum CGRP levels and markedly higher serum levels of proinflammatory cytokines after LPS administration, compared with their wild-type (WT) counterparts. Dysregulation of proinflammatory cytokine levels in RAMP1-/- mice is attributed to deficient signal transduction by CGRP in dendritic cells, suggesting that CLR/RAMP1 receptors regulate not only blood pressure but also inflammatory responses.

We have reported (8-10) that gastrointestinal tracts contain a large amount of CGRP and experience the protective actions from the effects of ethanol, a harmful necrotizing agent. Recently, we found that CGRP also exhibits proangiogenic activity in models of cancer and hindlimb ischemia (11, 12). These studies suggested that CGRP functions as an intermediate between vascular and neuronal systems under pathological conditions. Further, we identified increased levels of CGRP during gastric ulcer healing that facilitate angiogenesis (13).

The establishment of a vascular supply is essential, not only for organ development and

differentiation during embryogenesis, but also for the process of wound healing (14). The formation of lymphatic vessels, or lymphangiogenesis, occurs during the development of the corpus luteum and during wound healing and may be increased in certain pathologic processes (15). It typically occurs at sites of inflammation induced by factors produced by macrophages. The process of lymphangiogenesis contributes to the reduction of tissue edema and activation of immune responses by facilitating fluid drainage and the transport of dendritic cells and macrophages (16-18). In the present study, we used RAMP1-/- mice to investigate the role of RAMP1 in lymphangiogenesis during the healing of skin wounds. The results showed that CLR/RAMP1 signaling plays a crucial role in wound healing and wound-induced angiogenesis and lymphangiogenesis and that it presents a promising target for controlling these processes in vivo.

2. Materials and Methods

2-1. Animals

RAMP1-/- mice were developed as described elsewhere (7). Male 8- to 10-week-old C57BL/6 WT mice and RAMP1-/- mice were used in this study. RAMP1-/- mice exhibit good health, show normal behavior, and have no visible phenotypes different from normal mice. All animals were housed individually under a 12-h light-dark cycle at a constant temperature (25 ± 1°C) and humidity (60 ± 5%). All mice had free access to tap water and rodent chow. All experiments were performed in accordance with the guidelines for animal experiments established by the Kitasato University School of Medicine.

2-2. Determination of expressions of pro-CGRP, CGRP, and RAMP1 in DRGs

The medulla spinalis was removed, and the DRGs of the L_{1-5} vertebrae were isolated. DRG tissues were homogenized in 1 ml of TRIzol reagent (Gibco-BRL; Life Technologies, Rockville, MD, USA). A sample of RNA was extracted from the tissue according to the manufacturer's instructions. Real-time PCR was performed as described below. The oligonucleotide primers were as follows: for pro-CGRP,
5′ -CCCCAGAATGAAGGTTACACA-3′ (sense) and
5′ -TGTCAAAGGGAGAAGGGTTTT-3′ (antisense); for CGRP,
5′ -CCCCAGAATGAAGGTTACACA-3′ (sense) and
5′ -TGTCAAAGGGAGAAGGGTTTT-3′ (antisense); and for GAPDH,
5′ -CCCTTCATTGACCTCAACTACAATGGT-3′ (sense) and
5′ -GAGGGGCCATCCACAGTCTTCTG-3′ (antisense).

2-3. Skin wound model and evaluation of the wound healing process

Surgical wounds were made on the backs of the mice, as described elsewhere (19). In brief, after the mice were anesthetized with pentobarbital sodium (50 mg/kg, i.p.), the dorsal hair was shaved, the exposed skin was cleaned with 70% ethanol, and full-thickness skin wounds of 6-mm diameter were made aseptically on either side of the dorsal midline. The day of surgical treatment was defined as day 0. Each wound region was digitally photographed at a fixed time, and the wound areas were calculated by Image J image analysis software (U.S. National Institutes of Health, Bethesda, MD, USA). Changes in wound area were expressed as a percentage of the wound area at day

0.

2-4. Immunohistochemistry

For immunohistochemistry, wound tissues were immediately fixed with 4% paraformaldehyde and stained with anti-CD31 antibody (1:500 dilution) and anti-lymphatic vessel endothelial hyaluronan receptor 1 (LYVE-1; 1:500 dilution), to identify blood and lymphatic vessels, respectively. Immune complexes were detected with an LSAB + System-HRP kit (DakoCytomation, Carpinteria, CA, USA). Wound-induced angiogenesis and lymphangiogenesis in granulation tissues were estimated by micro blood vessel density and lymphatic vessel density and expressed as the number of vessels per square millimeter.
For immunofluorescence, the primary antibodies used were anti-RAMP1 antibody (1:100 dilution), CD31 (1:500 dilution), CD11b (1:200 dilution), and S100A4 (1:200 dilution). Images were captured with a confocal scanning laser microscope (LSM700; Zeiss, Jena, Germany), and computer-assisted morphometric analyses were performed with ZEN 2008 software (Zeiss).

2-5. Collection and culture of peritoneal macrophages

Peritoneal macrophages were obtained from 8- to 10-week-old WT mice and RAMP1-/- mice that had received 2 ml of thioglycolate i.p. 3 days earlier. The macrophages were washed, resuspended, placed in 12-well culture plates (1×10^6/well), and treated for 24 h in RPMI 1640 medium (Cambrex, Baltimore, MD, USA), containing 10% FBS at 37°C in 5% humidified CO_2. After 24 h, the plates were washed with phosphate-buffered saline (PBS) to remove nonadherent cells. Approximately 60% of the cells remained adherent and were used in all subsequent experiments.

2-6. Real-time RT-PCR

Transcripts encoding CD31, vascular endothelial growth factor (VEGF)-A, VEGF-C, VEGFR-3, epidermal growth factor (EGF), transforming growth factor (TGF)-ß, basic fibroblast growth factor (bFGF), connective tissue growth factor (CTGF), and glyceraldehyde-3-phosphate dehydrogenase (GAPDH) were quantified by real-time RT-PCR analysis. Total RNA was extracted from mouse tissues with TRIzol (Gibco-BRL), and single-stranded cDNA was generated from 1 μg of total RNA via reverse transcription with ReverTra Ace-α (Toyobo, NewYork, NY, USA). Quantitative

PCR amplification was performed with SYBR Premix Ex Taq (Takara Bio, Shiga, Japan) and the following gene-specific primers:
5'-ACTTCTGAACTCCAACAGCGA-3' (sense) and
5'-CCATGTTCTGGGGGTCTTTAT-3' (anti-sense) for CD31,
5'-GAGAGAGGCCGAAGTCCTTT-3' (sense) and
5'-TTGGAACCGGCATCTTTATC-3' (anti-sense) for VEGF-A,
5'-TCTGTGTCCAGCGTAGATGAG-3' (sense) and
5'-GTCCCCTGTCCTGGTATTGAG-3' (anti-sense) for VEGF-C,
5'-CCTATTGACATGCTGTGGGAT-3' (sense) and
5'-GTGGGTTCCTGGAGGTAAGAG-3' (anti-sense) for VEGF-D,
5'-TTTATGTCCCACCCCCACTAC-3' (sense) and
5'-GGCTGAGCTACAAGGCAATCG-3' (anti-sense) for VEGFR-3,
5′ -ATGGGAAACAATGTCACGAAC-3′ (sense) and
5′ -TGTATTCCGTCTCCTTGGTTC-3′ (anti-sense) for EGF,
5′ -AACAATTCCTGGCGTTACCTT-3′ (sense) and
5′ -TGTATTCCGTCTCCTTGGTTC-3′ (anti-sense) for TGF-β,
5′ -GGCTGCTGGCTTCTAAGTGTG-3′ (sense) and
5′ -TTCCGTGACCGGTAAGTATTG-3′ (anti-sense) for bFGF,
5′ -AACCGGGGAGGGAAATTATAG-3′ (sense) and
5′ -TGGAATCAGAATGGTCAGAGG-3′ (anti-sense) for CTGF,
5'-ACATCAAGAAGGTGGTGAAGC-3' (sense) and
5'-AAGGTGGAAGAGTGGGAGTTG-3' (anti-sense) for GAPDH. The obtained threshold cycle (C_t) values were processed for further calculations according to the comparative C_t method. Expression levels of target genes were normalized to the housekeeping gene GAPDH, giving the ΔC_t value. Finally, the gene expression level was calculated as $2^{-\Delta Ct}$, giving the final value that was normalized to that of the housekeeping gene.

2-7. RT-PCR analysis in macrophages

Thioglycolate-induced macrophages were incubated for 4 h with CGRP (3 and 30 nM) and RPMI 1640 medium. Next, the macrophages were collected, and mRNA was isolated with Trizol reagent (Life Technologies-Invitrogen, Carlsbad, CA, USA). Expression levels of VEGF-A and VEGF-C mRNA in macrophages were measured by real-time RT-PCR.

2-8. RT-PCR analysis in fibroblasts

Murine fibroblasts (L929) were obtained from the Cell Bank, RIKEN Bioresource Center (Ibaraki, Japan). The cells were cultured in DMEM supplemented with 10% (v/v) FBS and 100 U/500 ml penicillin (GIBCO-BRL) at 37°C in 5% humidified CO_2. L929 fibroblasts (3×10^5 cells/well) were incubated for 6 h with CGRP (3 and 30 nM) and PBS, and the mRNA expression levels of VEGF-A, VEGF-C and VEGF-D in fibroblasts were determined by real-time RT-PCR.

2-9. Drainage of fluorescein isothiocyanate–dextran from wound areas

At 7 days after wounding, 200 µl of 3% fluorescein isothiocyanate–dextran was injected s.c. into the wound granulation tissues. At 2 h after the injections, axillary lymph nodes were excised to measure the intensity of fluorescence drained from the wound area via newly formed lymphatic vessels. A Nano Drop 3300 Fluorospectrometer (Thermo Scientific, Wilmington, DE, USA) was used to quantitate the intensity of the fluorescence of the extracted dye.

2-10. Murine bone marrow transplantation (BMT) model

Bone marrow (BM) cells were obtained by flushing the cavities of freshly dissected femurs and tibiae from donor male RAMP1-/- mice with PBS. Donor BM cells were harvested from their WT counterparts (8-week-old male C57BL/6 mice) by the same method. The flushed BM cells of each donor were dispersed by pipetting and resuspended in PBS at a density of 1×10^7 cells/ml. WT mice were lethally irradiated at 9.0 Gy, with an MBR-1505R X-ray irradiator (Hitachi Medico Co., Tokyo, Japan) with a filter (copper, 0.5 mm; aluminum, 2 mm) monitoring the cumulative radiation dose. Donor BM mononuclear cells (2×10^6 cells) in 200 µl of PBS were transplanted via the tail vein of irradiated WT mice. After 12 weeks, peripheral blood was collected, and RAMP1 expression was tested to confirm chimerism.
GFP transgenic mice (a gift from Dr. M. Okabe, Genome Information Research Center, Osaka University, Osaka, Japan) with a C57BL/6 background were used as WT mice to confirm the chimerism. The mice, in which >95% of the peripheral leukocytes exhibited GFP positivity in fluorescence-activated cell-sorting analysis, were used in this experiment as the control group.

2-11. Denervation of sciatic nerves

Unilateral denervation of the sciatic nerve was performed in mice under pentobarbital sodium anesthesia (25 mg/kg). The sciatic nerves (L_{1-5}) were exposed through a gluteus muscle incision, and 5 mm of the sciatic nerve distal to the DRG was removed. The operated region was marked with a polypropylene suture (6-0; Ethicon) with the aid of an operating microscope. Sham-operated mice were prepared as controls with the same operation but without the sciatic nerve axotomy. After confirming the delay in escape from the heat, surgical wounds were made on the backs of hind limb, as described previously (11).

2-12. Chemical denervation

Neonatal mice (WT) were given subcutaneously with capsaicin at doses of 50 mg/kg. Eight weeks after the capsaicin treatment, wounds were made on the back of the mice, and wound healing process was determined as described above.

2-13. Statistical analysis

Data are expressed as means ± SEM. Comparisons among multiple groups were performed via factorial analysis of variance (ANOVA), followed by Scheffe's test. Comparisons between 2 groups were performed with the Mann-Whitney U test. Values of $P < 0.05$ were considered statistically significant.

3. Results

3-1. Suppression of wound-induced angiogenesis in RAMP1-/- mice

The RAMP1-/- mice appeared healthy, and their small size was the same as that of their WT counterparts. The basal levels of mRNAs of pro-CGRP and CGRP in the DRG tissues in the non-treated RAMP1-/- mice were not different from those in WT (Fig. 1 A, B), suggesting that the CGRP levels in the neuronal system were not reduced in RAMP1-/-. By contrast, the RAMP1 expressed in the DRGs was much lower in the RAMP1-/- mice in comparison with the WT (Fig. 1C). These results suggest that RAMP1-/- mice are good tools for evaluating the CGRP signaling in pathologic conditions.

Full-thickness skin wounds were surgically created on the backs of WT mice, and the closure of the wounds was monitored. The healing process observed in this mouse model occurred in a manner essentially the same as the process reported previously. At 24 h after wounding, the wound areas were reduced to 50% in the control WT mice, and the wounds were completely closed after 13 days. Invasion of granulation tissue from the wound margins into the wound bed was observed 2 days after injury. At day 3, the wound bed was filled completely with granulation tissue, and at this stage, marked neovascularization was evident.

To evaluate the roles of endogenous CGRP-RAMP1 signaling in wound-dependent angiogenesis and wound closure, we created skin wounds in both RAMP1-/- mice and WT mice, and monitored the healing process for 14 days. As shown in Fig. 1D, E, wound closure in the RAMP1-/- mice was significantly delayed compared with that in the WT mice, especially during the early phase of the healing process.

At days 2, 3, 4, 5, 6, and 7, we compared the histologic appearance of wounds in the WT and RAMP1-/- mice. Although immunostaining of CD31-positive microvessels indicated the presence of abundant microvessel assemblies in the wound granulation tissues (Fig. 2B) of the WT mice, few were observed in the RAMP1-/- mice (Fig. 2B, C). Moreover, the RAMP1-/- mice demonstrated significantly lower microvessel densities throughout the observation periods than did the WT mice (Fig. 2D). Real-time RT-PCR analysis also showed significantly lower CD31 and VEGF-A mRNA levels in the RAMP1-/- mice than in the WT mice during the early phase of the healing process (days 2, 5, and 7 for CD31; days 2, and 3 for VEGF-A, Fig. 2E, F). When the expressions of other cytokines were determined in the wound granulation tissues, TGF-β, bFGF, and CTGF were also reduced in the early stage of wound healing in the RAMP1-/- mice, whereas there was no marked reduction in EGF (Fig. 6). These results suggest that endogenous

CGRP-RAMP1 signaling up-regulates angiogenesis in the wound granulation tissues by inducing the growth factors including VEGF-A, and thereby facilitates wound healing.

To examine the localization of RAMP1 in the endothelial cells (ECs), we performed double immunostaining of RAMP1 and CD31 (Fig. 2A). No RAMP1/CD31 double-positive vessels were observed in granulation tissues, although they were present in uninjured lesions around the wounds. This observation indicates that newly formed vessels in granulation tissues lack RAMP1 expression. These results suggest that CGRP-RAMP1 signaling does not play a direct role in forming new vessels.

3-2. Cellular components relevant to CGRP-RAMP1 signaling-dependent angiogenesis

To identify the cells responsible for enhancing wound-induced angiogenesis via CGRP-RAMP1 signaling, we evaluated macrophages and fibroblasts, the 2 major components of wound granulation tissues. We performed double immunostainings of RAMP1 and CD11b, a macrophage marker (Fig. 3A), and of RAMP1 and S100A4, an activated fibroblast marker (Fig. 3B) in granulation tissues 7 days after wounding. A large number of CD11b- and S100A4-positive cells were found to express RAMP1. We then tested the in vitro effects of CGRP on macrophages and fibroblasts. When mouse fibroblasts (L929 cells) were treated with CGRP agonists, no increase in VEGF-A expression was observed (Fig. 3F). By contrast, VEGF-A expression increased in macrophages isolated from the peritoneal cavities of WT mice in a dose-dependent manner when treated with CGRP agonists (Fig. 3C). These results suggest that CGRP-RAMP1 signaling up-regulates angiogenesis in granulation tissues by inducing VEGF-A expression in macrophages.

Furthermore, we tested whether lymphangiogenic factors increase in response to CGRP agonists. Neither VEGF-C nor VEGF-D production was significantly enhanced in L929 cells (Fig. 3G, H). In macrophages, VEGF-C expression increased, whereas VEGF-D expression did not (Fig. 3D, E). These results suggest that CGRP-RAMP1 signaling up-regulates lymphangiogenesis in granulation tissues by inducing VEGF-C in macrophages, but not in fibroblasts.

3-3. Suppression of wound-induced lymphangiogenesis in RAMP1-/- mice

On days 3, 5, 6, 7, and 10, we compared the histologic appearance of the wounds in the WT and RAMP1-/- mice, to evaluate lymphangiogenesis in granulation tissues. Immunohistochemical analysis with an antibody to the lymphatic-specific marker

LYVE-1 revealed fewer LYVE-1-positive lymphatic structures in the RAMP1-/- mice than that in the WT mice (Fig. 4B, C). Moreover, quantitative analysis of lymphatic vessel density confirmed that wound-induced lymphangiogenesis in the RAMP1-/- mice was significantly reduced at days 6, 7, and 10 compared with that in the WT mice (Fig. 4D). Real-time RT-PCR analysis also showed significantly lower VEGF-C and VEGFR-3 mRNA levels in the RAMP1-/- mice than in the WT mice from early phases of the healing process (Fig. 4E, F). These results suggest that lymphangiogenesis in wound granulation tissues is accelerated by VEGF-C and VEGFR-3 signaling from early stages and is dependent on endogenous CGRP-RAMP1 signaling. In addition, as shown in Fig. 4G, H, the drainage of fluorescent dye injected into the wound area into the regional lymph nodes (axillary lymph nodes) was reduced in the RAMP1-/- mice at day 7, when lymphangiogenesis was suppressed in the mice. Therefore, lymphangiogenesis appears to modulate lymphatic flow in the granulation tissues with newly formed lymphatic vessels via a CGRP-dependent mechanism.

To examine the localization of RAMP1 in lymphatic ECs, we performed double immunostaining for RAMP1 and LYVE-1 (Fig. 4A). No RAMP1 and LYVE-1 double-positive vessels were observed in granulation tissues, indicating that newly formed lymphatic vessels in granulation tissues do not express RAMP1. These results suggest that CGRP-RAMP1 signaling does not directly affect newly formed lymphatic vessels, rather, it up-regulates lymphangiogenesis by inducing VEGF-C expression in macrophages.

3-4. Role of recruited BM cells expressing RAMP1 in wound healing

Recent results suggest that recruitment of hematopoietic cells from the BM plays a crucial role in wound healing. We next examined the role of recruited BM cells expressing RAMP1 in wound-induced angiogenesis and lymphangiogenesis. In comparison with mice with transplanted WT BM cells, mice with BM cells transplanted from RAMP1-/- mice demonstrated significantly delayed wound healing, especially during the early phase of the healing process (Fig. 5A). A reduced accumulation of RAMP1-postive cells was observed at day 7 after wounding in the wound granulation tissues of mice with BM cells transplanted from RAMP1-/- mice (Fig. 7A, B). Immunohistochemical analysis with a CD31 antibody showed that microvessel density at day 3 after wounding in mice with BM cells transplanted from RAMP1-/- mice was significantly suppressed compared with mice receiving WT BM cells (Fig. 5B, C). Immunohistochemical analysis with a LYVE-1 antibody revealed significantly decreased lymphatic vessel density at day 7 after wounding in mice with BM cells

transplanted from RAMP1-/- mice, compared with mice receiving WT BM cells (Fig. 5D, E).

Histologically, GFP-positive cells accumulated in the wound granulation tissues in the wound granulation tissues in the WT mice with BM cells transplanted from GFP-transgenic mice with a C57BL/6 background, suggesting that transplanted BM cells were recruited into the wound granulation tissues. When we performed immunostaining of RAMP1, CD11b, and S100A4 in the granulation tissues of mice with BM cells transplanted from GFP-transgenic mice 7 days after wounding, a large number of GFP and RAMP1 double-positive cells and GFP and CD11b double-positive cells were observed in the tissues (Fig. 7C, D). These results suggest that macrophages from the BM are recruited into inflammatory lesions, where they appear to secrete VEGF-A and VEGF-C in response to CGRP stimulation, thereby contributing to angiogenesis and lymphangiogenesis.

In separate experiments, we confirmed that neuronal system-derived CGRP was relevant to RAMP1 stimulation during the healing process of this model. The wound healing processes and angiogenesis/lymphangiogenesis in WT mice denervated either surgically or chemically, in which CGRP release to the peripheral tissues may be reduced, were suppressed in comparison with those in sham-surgery mice and vehicle-treated mice (Fig. 8A-E). These strengthen the significance of RAMP1 signaling in the wound healing processes.

4. Discussion

CGRP is a 37-aa neuropeptide released in response to sensory stimuli that contributes to various biological processes, such as cardiovascular regulation and vasodilation (20). Using the peptidic antagonist CGRP (8–37) and the antagonist BIBN4096BS, pharmacologic researchers have classified CGRP receptors into 2 subtypes: CGRP-1 and CGRP-2 (21, 22). Although more CGRP receptor subtypes have been suggested, only one receptor, CLR, which belongs to a large family of GPCRs, has been identified molecularly (23). This receptor of the B-family of GPCRs forms a heterodimer with a single transmembrane domain protein, RAMP. Three distinct RAMPs have been cloned and been shown to determine the selectivity of the CRLR-receptor for the different members of the calcitonin/CGRP family of peptides (24). Co-expression of CLR with RAMP1 results in formation of the CGRP receptor, whereas co-expression of CLR with RAMP2 or RAMP3 corresponds to the formation of AM1 or AM2 receptors, respectively (24). CGRP binds to the AM2 receptor with ～50-fold lower affinity than does AM and has an even lower affinity for AM1 receptors (24). This suggests that RAMP1 is the key receptor for supporting CGRP activity and that a RAMP1-null mouse model is a good tool for clarifying the roles of CGRP and RAMP1 in vivo.

In the present experiment, we used RAMP1-/- mice to define the roles of RAMP1 in angiogenesis and lymphangiogenesis during wound healing. As shown in Fig. 2C-E, angiogenesis in the granulation tissues in the base of the wounds was suppressed from the early stages in the RAMP1-/- mice in comparison with that in their WT counterparts. Expression of RAMP1 in vascular ECs in granulation tissues in the WT mice was faint compared with the expression observed in established blood vessels in normal mouse skin. The potent hypotensive action of CGRP is explained by the stimulation of CGRP receptor in which RAMP1 commits as a cofactor for the intracellular signaling.

The low level of RAMP1 expression in neovascularized blood vessels was a surprising observation. It has been frequently reported that microvascular ECs display a large degree of functional heterogeneity, depending on their location in the vascular tree (25). The existence of organ-specific, microvascular-bed-specific, and even intravascular variations in endothelial cell gene expression emphasizes their high cell-to-cell variability, which allows them to adapt to changing conditions. Further, the ability of microvascular ECs to respond dynamically to pathology-related microenvironmental changes is particularly apparent with respect to angiogenesis. The present study demonstrates that the site of CGRP activity and the localization of RAMP1 in neovascularized areas are different than in vascular ECs. Newly formed blood vessels

in a pathologic setting may be quite different from the mature blood vessels formed during development and tissue maintenance and homeostasis.

The major cellular components of wound granulation tissues relevant to healing and angiogenesis are fibroblasts and macrophages (19). Both fibroblasts and macrophages express RAMP1, but when cultured fibroblasts were incubated with CGRP, no increase in the expression of VEGF isoforms was observed (Fig. 3F-H). By contrast, when exposed to CGRP, macrophages isolated from the mouse peritoneal cavity exhibited increased expression of VEGF-A and VEGF-C, but not VEGF-D, in a dose-dependent manner (Fig. 3C-E). VEGF-A is active in this model, since the addition of a VEGF neutralizing antibody or VEGF receptor tyrosine kinase inhibitor strongly inhibits proangiogenic processes (26). Furthermore, VEGF-C is a potent inducer of lymphangiogenesis (27). LYVE-1-positive cells did not express RAMP1, indicating that lymphatic ECs do not express RAMP1 in the same manner as neovascularized vascular ECs. Newly formed lymphatics also failed to exhibit RAMP1 expression, suggesting that the important cellular components are non-ECs, such as macrophages. VEGF-C reduction was seen in the RAMP1-/- from the early stages of the healing. Thus, it appears that lymphangiogenesis, as seen in the present study, may be regulated by VEGF-C released from macrophages in the early stages.

The established lymphatic vessels observed in this study effectively drained the interstitial fluids, as demonstrated by the movement of dye injected subcutaneously (Fig. 4G, H). AM induces lymphangiogenesis (28), and the presence of the AM receptor on lymphatic ECs is reported, suggesting that the cellular components necessary for RAMP1 signaling are different from those needed for AM activity. Immunohistochemical staining revealed that RAMP1 expression co-localized with CD11b expression, suggesting that macrophages actively induce lymphangiogenesis in granulation tissues in the wound base. This is the first report describing the involvement of RAMP1 expressed by macrophages in enhancing angiogenesis and lymphangiogenesis in vivo. Controlling RAMP1 signaling is a good option for the treatment of angiogenesis/lymphangiogenesis-related pathologic conditions. In addition, recruited macrophages were shown to be crucial for angiogenesis/lymphangiogenesis, since RAMP1-/- BM chimeric mice exhibited decreased angiogenesis and lymphangiogenesis in wound granulation tissues and showed delayed wound healing (Fig. 5).

Activation of the CGRP receptor results in Gαs-mediated activation of AC with a subsequent increase in cAMP and activation of nitric oxide synthase (NOS), both of which are closely related to vasodilatation (29-32). We previously reported that cAMP elevation up-regulated the expression of VEGF and enhanced angiogenesis in a sponge

implantation model (33). Forskolin, which activates AC, enhanced angiogenesis, and the phosphodiesterase inhibitor amrinone, which induces the accumulation of intracellular cAMP, increased neovascularization in sponge granulation tissues (33). These intracellular signaling cascades have been shown to couple CGRP receptors related to physiological responses, such as vasodilatation of blood vessels. This study confirmed that CGRP receptor signaling relevant to cAMP elevation increased pathologic angiogenesis and is responsible for increasing VEGF expression in hematopoietic cells such as macrophages (Fig. 3C, D), consistent with a previous in vitro report (34).

In the present study, we did not measure the amount of CGRP released. However, we have characterized the release of CGRP in angiogenic responses under pathologic conditions in previous reports (8, 11-13). Healing of skin wounds in neonatal mice was suppressed by capsaicin treatment, which depletes CGRP from sensory nerve endings (35). We had confirmed the effects of chemical denervation in the WT mice used in this study (Fig. 8E). C-fibers, which contain CGRP in their nerve endings, may be relevant to RAMP1-mediated neovascularization. In fact, surgical denervation of primary sensory neurons resulted in reduced angiogenesis and lymphangiogenesis (Fig. 8A-D). Further, in our previous reports, CGRP enhanced the healing of gastric ulcers, with substantial induction of angiogenesis in the ulcer base tissues (13), and recovery from hindlimb ischemia induced by the ligation of femoral arteries was augmented by the release of CGRP from the sensory nerves (12). In these instances, it is plausible to hypothesize that C-fibers were stimulated to release CGRP by proton ions secreted from the gastric mucosa or by ischemia, suggesting that the release of CGRP in such pathologic settings plays a significant role in enhancing angiogenesis. RAMP1 may be an element that is responsible for CGRP released during pathologic processes.

The functional and morphologic relationships between primary afferent neurons and blood vessels in pathologic conditions, such as ischemia and cancer development, are poorly understood. However, recent evidence suggests that the physical and biochemical interactions between these peripheral components are important in tumor biology and cancer-associated pain (36). Angiogenesis is a critical determinant for tumor growth, and an angiogenic switch, which allows the tumor to receive an adequate blood supply, is activated in the quiescent vasculature around tumors, contributing to tumor growth and metastasis, and ultimately decides a patient's prognosis. The neuronal system plays a fundamental role in the maturation of primitive embryonic vasculature. Mutations that disrupt peripheral sensory nerves or Schwann cells prevent proper arteriogenesis, whereas those that disorganize the nerves result in arteries with misrouted axons (37). It is also reported that sensory

neurons modulate the expression of arterial markers on ECs via the secretion of VEGF 164/120. These data suggest that during development, peripheral nerves play a role in determining organ-specific patterns of blood vessel branching and arterial maturation (38).

Some neuronal factors, such as Notch, are also reported to contribute to pathologic angiogenesis. Specialized ECs called tip cells, which lead and guide sprouting, share many features with another guidance structure, the axonal growth cone (39). Axonal growth cones and endothelial tip cells both respond to signals originating from the same molecular families, such as Slits and Roundabouts, Netrins and UNC5 receptors; Semaphorins, Plexins and Neuropilins; and Eph receptors and ephrin ligands. Activation of the Notch pathway and VEGF signaling induces angiogenic growth of ECs and the selection of tip cells, and Notch signaling is a key pathway that is activated during ischemia-induced neovascularization (40). Indeed, Notch signaling regulates several steps of the reparative process in ischemic tissues, including sprouting angiogenesis, vessel maturation, interaction of vascular cells with leukocytes, and skeletal myocyte regeneration. Together with findings in our previous studies, the present results suggest that CGRP has a major role in pathologic angiogenesis (11-13). Thus, RAMP1 is also a major player in these interactions. Thus, renewed focus should be placed on the interactions that occur between the neuronal systems and the lymphatic systems in pathologic conditions.

As discussed above, the findings in the present study indicate that both angiogenesis and lymphangiogenesis are enhanced by RAMP1 signaling in wound granulation tissues. RAMP1 was not expressed on ECs or lymphatic ECs during neovascularization. RAMP1 signaling was relevant to the expression of VEGF isoforms in macrophages derived from the BM, as tested in RAMP1-/- BM chimeric mice. Unlike AM-null mice, which exhibit edema during development, RAMP1-null mice are healthy, with no evidence of edema formation. Pathologic lymphangiogenesis was hampered in RAMP1-/- mice, as was drainage of interstitial fluids. The findings presented in this study indicate that RAMP1 signaling holds therapeutic potential for the treatment of pathologic angiogenesis/lymphangiogenesis-related conditions.

5. Acknowledgements

The authors thank Michiko Ogino, Kyoko Yoshikawa, Mieko Hamano and Yoshihiro Nara for technical assistance. This study was supported by the Integrative Research Program of the Graduate School of Medical Science at Kitasato University. The authors declare no conflicts of interest.

6. References

1. Morfis M, Christopoulos A, Sexton PM: RAMPs: 5 years on, where to now? Trends in pharmacological sciences 2003; 24:596-601.
2. McLatchie LM, Fraser NJ, Main MJ, Wise A, Brown J, Thompson N, et al: RAMPs regulate the transport and ligand specificity of the calcitonin-receptor-like receptor. Nature 1998; 393:333-9.
3. Deng PY, Li YJ: Calcitonin gene-related peptide and hypertension. Peptides 2005; 26:1676-85.
4. Kadmiel M, Fritz-Six KL, Caron KM: Understanding RAMPs through genetically engineered mouse models. Advances in experimental medicine and biology 2012; 744:49-60.
5. Hinson JP, Kapas S, Smith DM: Adrenomedullin, a multifunctional regulatory peptide. Endocrine reviews 2000; 21:138-67.
6. Steiner S, Muff R, Gujer R, Fischer JA, Born W: The transmembrane domain of receptor-activity-modifying protein 1 is essential for the functional expression of a calcitonin gene-related peptide receptor. Biochemistry 2002; 41:11398-404.
7. Tsujikawa K, Yayama K, Hayashi T, Matsushita H, Yamaguchi T, Shigeno T, et al: Hypertension and dysregulated proinflammatory cytokine production in receptor activity-modifying protein 1-deficient mice. Proceedings of the National Academy of Sciences of the United States of America 2007; 104:16702-7.
8. Boku K, Ohno T, Saeki T, Hayashi H, Hayashi I, Katori M, et al: Adaptive cytoprotection mediated by prostaglandin I(2) is attributable to sensitization of CRGP-containing sensory nerves. Gastroenterology 2001; 120:134-43.
9. Saeki T, Ohno T, Boku K, Saigenji K, Katori M, Majima M: Mechanism of prevention by capsaicin of ethanol-induced gastric mucosal injury--a study in the rat using intravital microscopy. Alimentary pharmacology & therapeutics 2000; 14 Suppl 1:135-44.
10. Arai K, Ohno T, Saeki T, Mizuguchi S, Kamata K, Hayashi I, et al: Endogenous prostaglandin I2 regulates the neural emergency system through release of calcitonin gene related peptide. Gut 2003; 52:1242-9.
11. Toda M, Suzuki T, Hosono K, Hayashi I, Hashiba S, Onuma Y, et al: Neuronal system-dependent facilitation of tumor angiogenesis and tumor growth by calcitonin gene-related peptide. Proceedings of the National Academy of Sciences of the United States of America 2008; 105:13550-5.
12. Mishima T, Ito Y, Hosono K, Tamura Y, Uchida Y, Hirata M, et al: Calcitonin gene-related peptide facilitates revascularization during hindlimb ischemia in

mice. American journal of physiology Heart and circulatory physiology 2011; 300:H431-9.
13. Ohno T, Hattori Y, Komine R, Ae T, Mizuguchi S, Arai K, et al: Roles of calcitonin gene-related peptide in maintenance of gastric mucosal integrity and in enhancement of ulcer healing and angiogenesis. Gastroenterology 2008; 134:215-25.
14. Singer AJ, Clark RA: Cutaneous wound healing. The New England journal of medicine 1999; 341:738-46.
15. Karpanen T, Alitalo K: Molecular biology and pathology of lymphangiogenesis. Annual review of pathology 2008; 3:367-97.
16. Baluk P, Tammela T, Ator E, Lyubynska N, Achen MG, Hicklin DJ, et al: Pathogenesis of persistent lymphatic vessel hyperplasia in chronic airway inflammation. The Journal of clinical investigation 2005; 115:247-57.
17. Kataru RP, Jung K, Jang C, Yang H, Schwendener RA, Baik JE, et al: Critical role of CD11b+ macrophages and VEGF in inflammatory lymphangiogenesis, antigen clearance, and inflammation resolution. Blood 2009; 113:5650-9.
18. Kerjaschki D: The crucial role of macrophages in lymphangiogenesis. The Journal of clinical investigation 2005; 115:2316-9.
19. Kamoshita E, Ikeda Y, Fujita M, Amano H, Oikawa A, Suzuki T, et al: Recruitment of a prostaglandin E receptor subtype, EP3-expressing bone marrow cells is crucial in wound-induced angiogenesis. The American journal of pathology 2006; 169:1458-72.
20. Amara SG, Jonas V, Rosenfeld MG, Ong ES, Evans RM: Alternative RNA processing in calcitonin gene expression generates mRNAs encoding different polypeptide products. Nature 1982; 298:240-4.
21. Quirion R, Van Rossum D, Dumont Y, St-Pierre S, Fournier A: Characterization of CGRP1 and CGRP2 receptor subtypes. Annals of the New York Academy of Sciences 1992; 657:88-105.
22. Dennis T, Fournier A, St Pierre S, Quirion R: Structure-activity profile of calcitonin gene-related peptide in peripheral and brain tissues. Evidence for receptor multiplicity. The Journal of pharmacology and experimental therapeutics 1989; 251:718-25.
23. Hay DL, Poyner DR, Quirion R, International Union of P: International Union of Pharmacology. LXIX. Status of the calcitonin gene-related peptide subtype 2 receptor. Pharmacological reviews 2008; 60:143-5.
24. Archbold JK, Flanagan JU, Watkins HA, Gingell JJ, Hay DL: Structural insights into RAMP modification of secretin family G protein-coupled receptors:

implications for drug development. Trends in pharmacological sciences 2011; 32:591-600.
25. Langenkamp E, Molema G: Microvascular endothelial cell heterogeneity: general concepts and pharmacological consequences for anti-angiogenic therapy of cancer. Cell and tissue research 2009; 335:205-22.
26. Amano H, Hayashi I, Endo H, Kitasato H, Yamashina S, Maruyama T, et al: Host prostaglandin E(2)-EP3 signaling regulates tumor-associated angiogenesis and tumor growth. The Journal of experimental medicine 2003; 197:221-32.
27. Jussila L, Alitalo K: Vascular growth factors and lymphangiogenesis. Physiological reviews 2002; 82:673-700.
28. Dunworth WP, Caron KM: G protein-coupled receptors as potential drug targets for lymphangiogenesis and lymphatic vascular diseases. Arteriosclerosis, thrombosis, and vascular biology 2009; 29:650-6.
29. Bell D, McDermott BJ: Calcitonin gene-related peptide in the cardiovascular system: characterization of receptor populations and their (patho)physiological significance. Pharmacological reviews 1996; 48:253-88.
30. Brain SD, Cambridge H: Calcitonin gene-related peptide: vasoactive effects and potential therapeutic role. General pharmacology 1996; 27:607-11.
31. Brown MJ, Morice AH: Clinical pharmacology of vasodilator peptides. Journal of cardiovascular pharmacology 1987; 10 Suppl 12:S82-7.
32. Preibisz JJ: Calcitonin gene-related peptide and regulation of human cardiovascular homeostasis. American journal of hypertension 1993; 6:434-50.
33. Amano H, Ando K, Minamida S, Hayashi I, Ogino M, Yamashina S, et al: Adenylate cyclase/protein kinase A signaling pathway enhances angiogenesis through induction of vascular endothelial growth factor in vivo. Japanese journal of pharmacology 2001; 87:181-8.
34. Zheng S, Li W, Xu M, Bai X, Zhou Z, Han J, et al: Calcitonin gene-related peptide promotes angiogenesis via AMP-activated protein kinase. American journal of physiology Cell physiology 2010; 299:C1485-92.
35. Toda M, Suzuki T, Hosono K, Kurihara Y, Kurihara H, Hayashi I, et al: Roles of calcitonin gene-related peptide in facilitation of wound healing and angiogenesis. Biomedicine & pharmacotherapy = Biomedecine & pharmacotherapie 2008; 62:352-9.
36. Mantyh PW, Clohisy DR, Koltzenburg M, Hunt SP: Molecular mechanisms of cancer pain. Nature reviews Cancer 2002; 2:201-9.
37. Mukouyama YS, Shin D, Britsch S, Taniguchi M, Anderson DJ: Sensory nerves determine the pattern of arterial differentiation and blood vessel branching in the

skin. Cell 2002; 109:693-705.
38. Miller G: Developmental biology. Nerves tell arteries to make like a tree. Science 2002; 296:2121-3.
39. Adams RH, Eichmann A: Axon guidance molecules in vascular patterning. Cold Spring Harbor perspectives in biology 2010; 2:a001875.
40. Al Haj Zen A, Madeddu P: Notch signalling in ischaemia-induced angiogenesis. Biochemical Society transactions 2009; 37:1221-7.

7. Figures

Figure 1

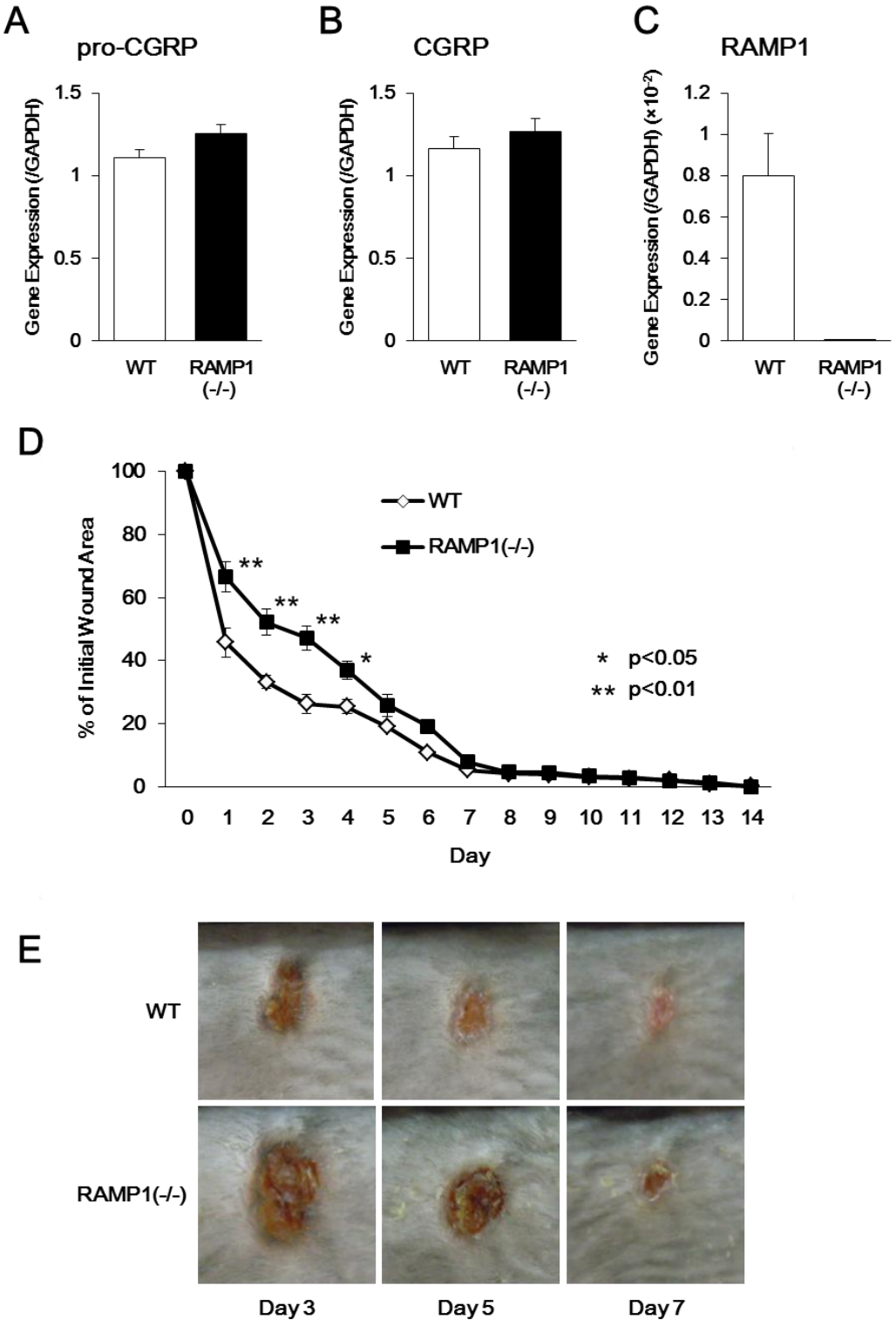

Figure 2-1

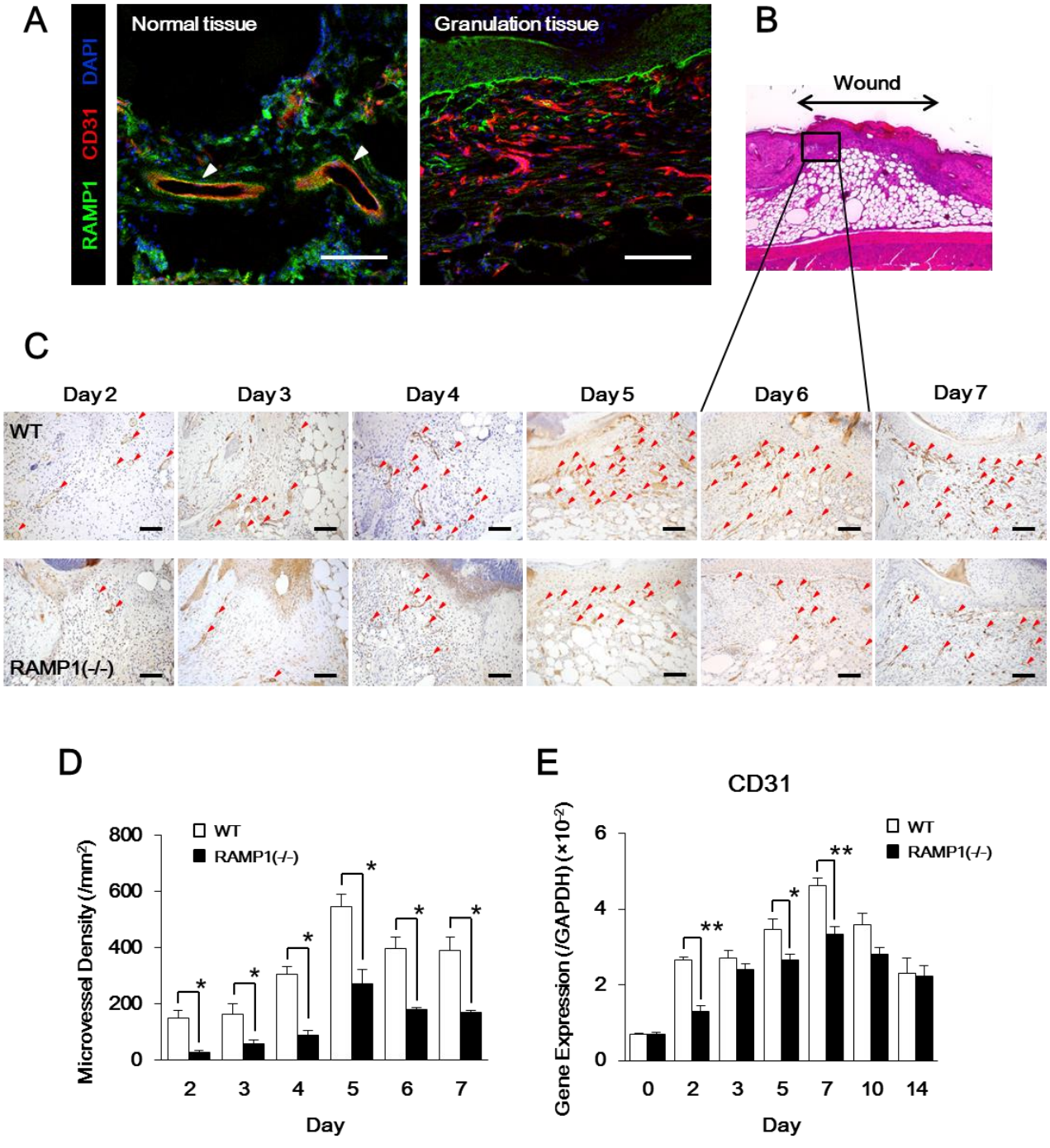
A
RAMP1 CD31 DAPI
Normal tissue
Granulation tissue
B
Wound
C
Day 2
Day 3
Day 4
Day 5
Day 6
Day 7
WT
RAMP1(-/-)
D
Microvessel Density (/mm²)
800
600
400
200
0
WT
RAMP1(-/-)
2
3
4
5
6
7
Day
E
CD31
Gene Expression (/GAPDH) (×10⁻²)
6
4
2
0
WT
RAMP1(-/-)
0
2
3
5
7
10
14
Day

Figure 2-2

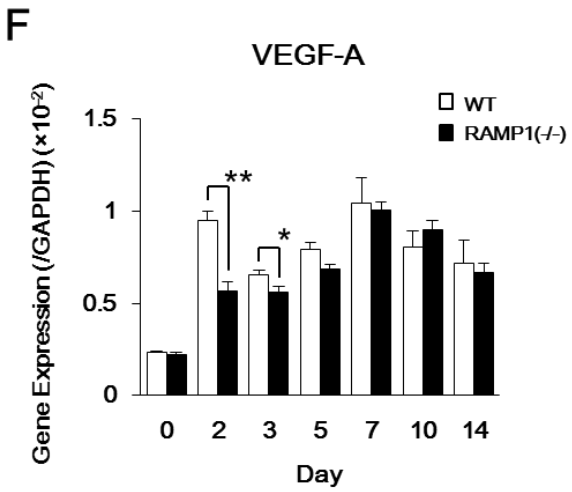
F
VEGF-A
WT
RAMP1(-/-)
Gene Expression (/GAPDH) (×10-2)
1.5
1
0.5
0
**
*
0
2
3
5
7
10
14
Day

Figure 3

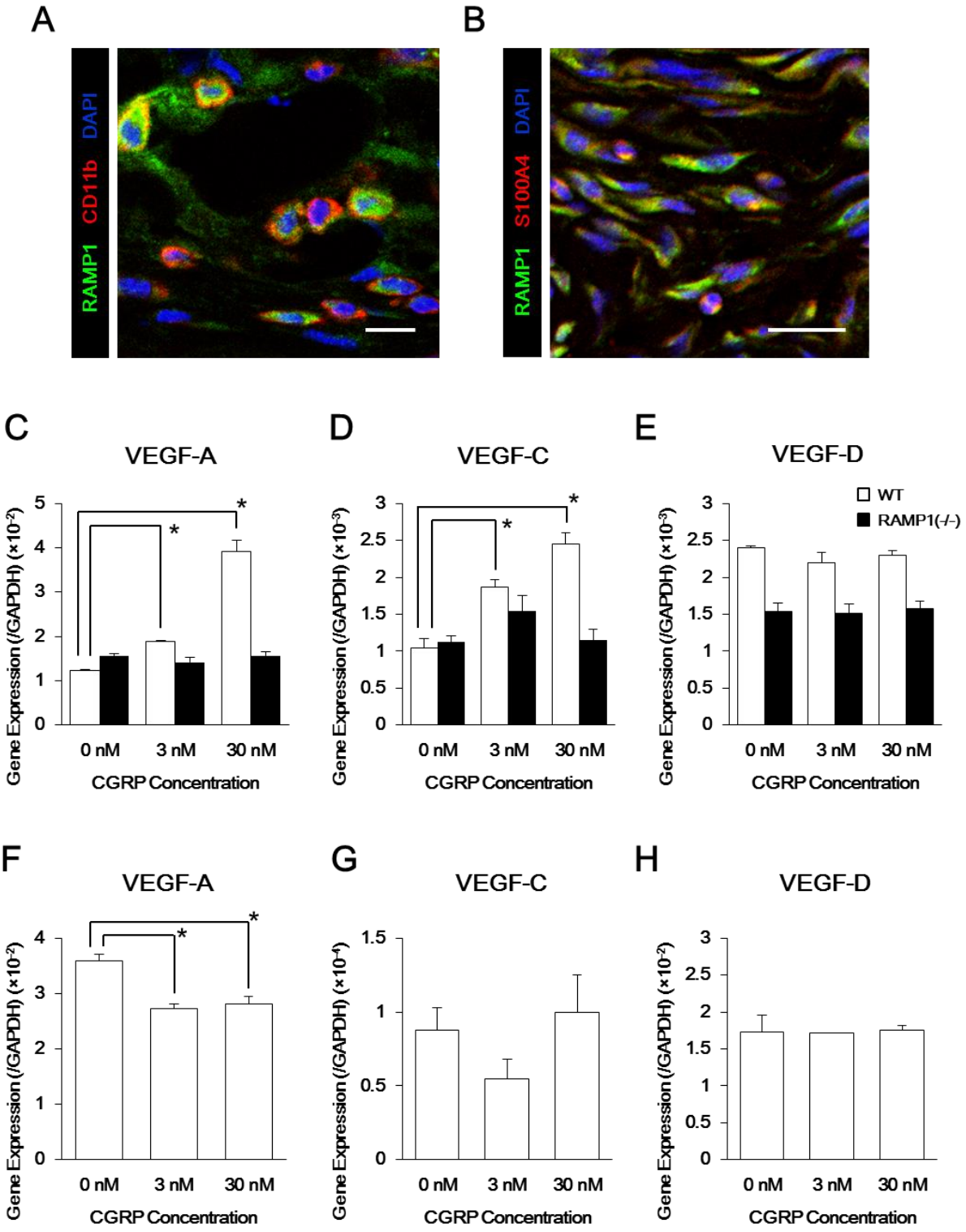
A
RAMP1 CD11b DAPI
B
RAMP1 S100A4 DAPI
C
VEGF-A
Gene Expression (/GAPDH) (×10-2)
0 nM 3 nM 30 nM
CGRP Concentration
D
VEGF-C
Gene Expression (/GAPDH) (×10-3)
0 nM 3 nM 30 nM
CGRP Concentration
E
VEGF-D
WT
RAMP1(-/-)
Gene Expression (/GAPDH) (×10-3)
0 nM 3 nM 30 nM
CGRP Concentration
F
VEGF-A
Gene Expression (/GAPDH) (×10-2)
0 nM 3 nM 30 nM
CGRP Concentration
G
VEGF-C
Gene Expression (/GAPDH) (×10-4)
0 nM 3 nM 30 nM
CGRP Concentration
H
VEGF-D
Gene Expression (/GAPDH) (×10-2)
0 nM 3 nM 30 nM
CGRP Concentration

Figure 4-1

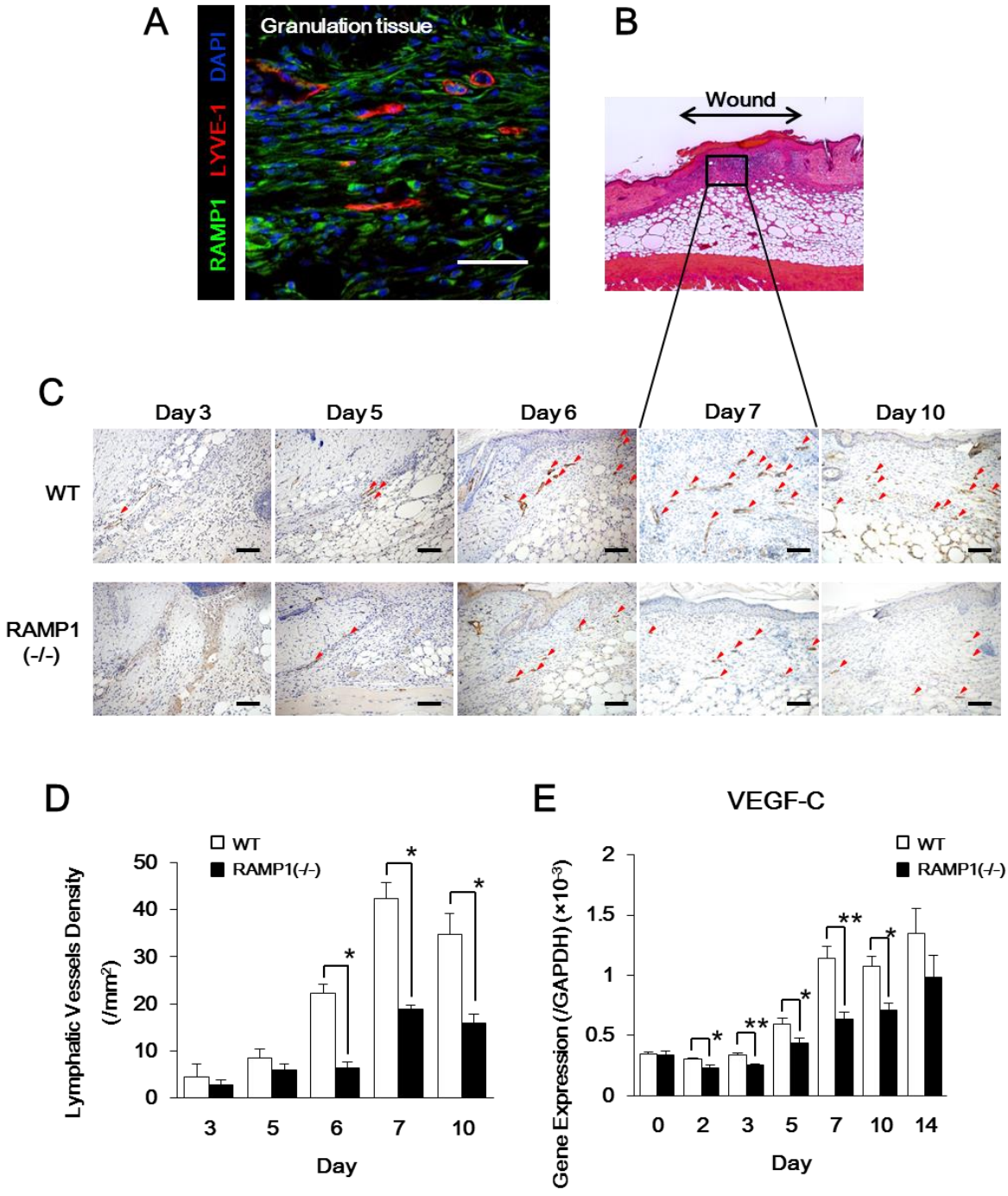
A
Granulation tissue
RAMP1 LYVE-1 DAPI
B
Wound
C
Day 3
Day 5
Day 6
Day 7
Day 10
WT
RAMP1 (-/-)
D
Lymphatic Vessels Density (/mm²)
WT
RAMP1(-/-)
Day
E
VEGF-C
Gene Expression (/GAPDH) (×10⁻³)
WT
RAMP1(-/-)
Day

Figure 4-2

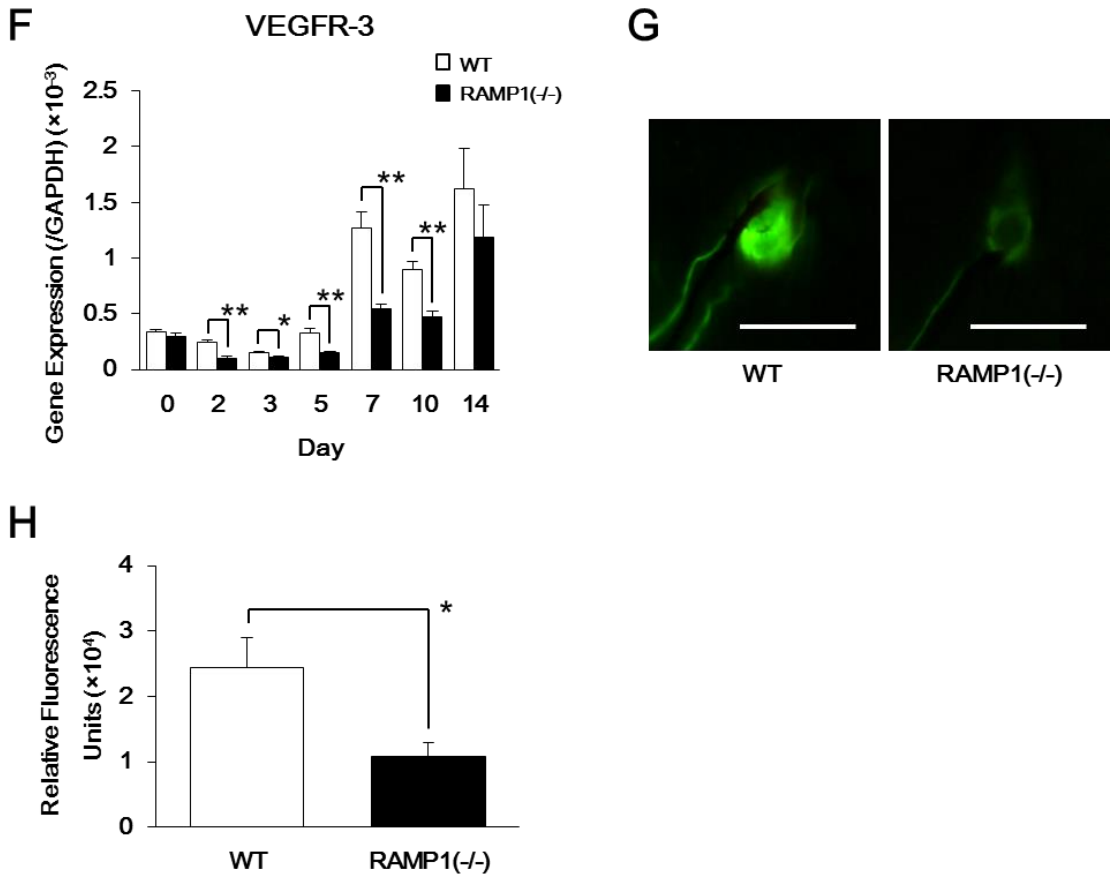
F
VEGFR-3
WT
RAMP1(-/-)
Gene Expression (/GAPDH) (×10-3)
2.5
2
1.5
1
0.5
0
0 2 3 5 7 10 14
Day
**
**
*
**
**
G
WT
RAMP1(-/-)
H
Relative Fluorescence Units (×10⁴)
4
3
2
1
0
*
WT
RAMP1(-/-)

Figure 5

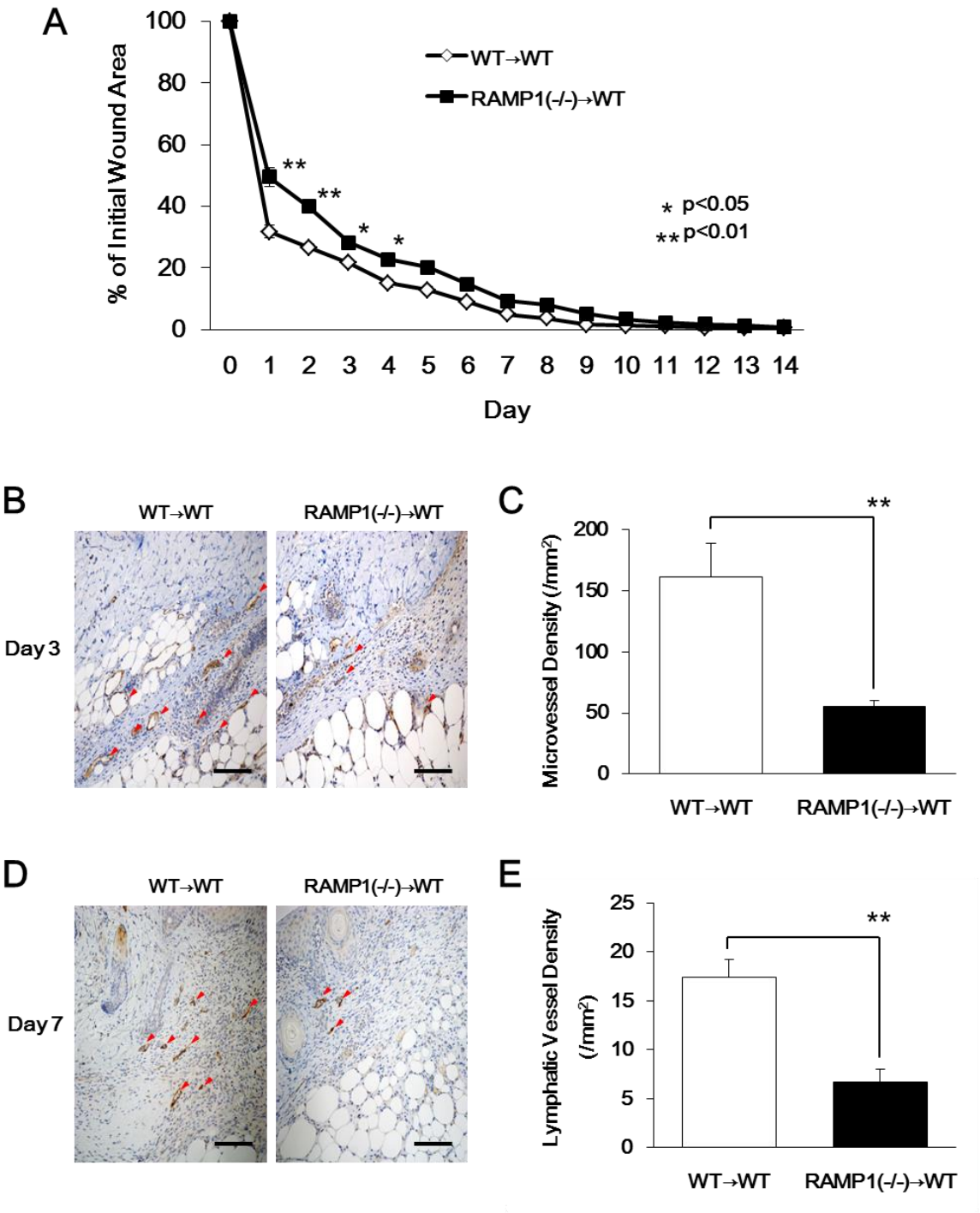
A
100
80
60
40
20
0
% of Initial Wound Area
WT→WT
RAMP1(-/-)→WT
**
**
*
*
* p<0.05
** p<0.01
0 1 2 3 4 5 6 7 8 9 10 11 12 13 14
Day
B
WT→WT
RAMP1(-/-)→WT
Day 3
C
**
200
150
100
50
0
Microvessel Density (/mm²)
WT→WT
RAMP1(-/-)→WT
D
WT→WT
RAMP1(-/-)→WT
Day 7
E
**
25
20
15
10
5
0
Lymphatic Vessel Density (/mm²)
WT→WT
RAMP1(-/-)→WT

Figure 6

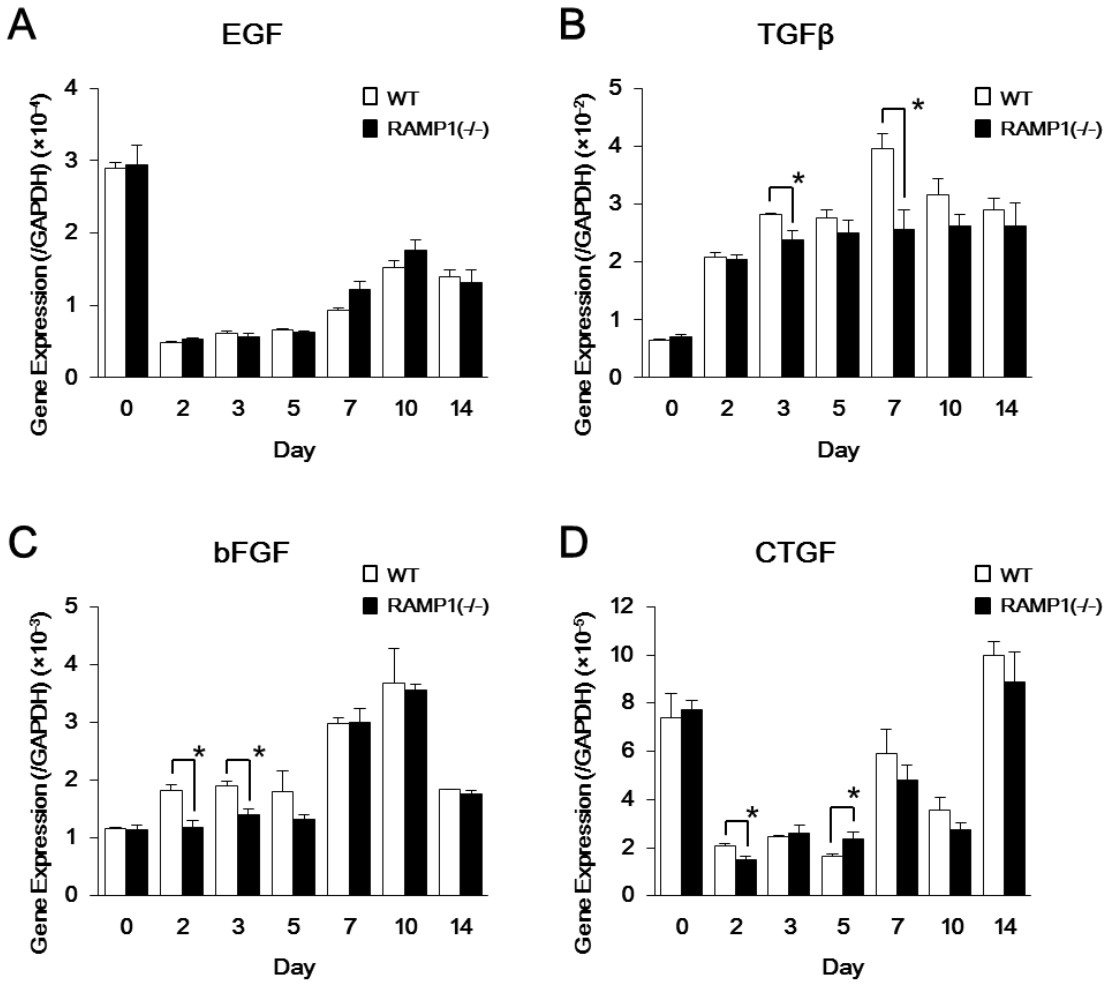
A
EGF
WT
RAMP1(-/-)
Gene Expression (/GAPDH) (×10⁻⁴)
0 1 2 3 4
0 2 3 5 7 10 14
Day
B
TGFβ
WT
RAMP1(-/-)
Gene Expression (/GAPDH) (×10⁻²)
0 1 2 3 4 5
*
*
0 2 3 5 7 10 14
Day
C
bFGF
WT
RAMP1(-/-)
Gene Expression (/GAPDH) (×10⁻³)
0 1 2 3 4 5
*
*
0 2 3 5 7 10 14
Day
D
CTGF
WT
RAMP1(-/-)
Gene Expression (/GAPDH) (×10⁻⁵)
0 2 4 6 8 10 12
*
*
0 2 3 5 7 10 14
Day

Figure 7

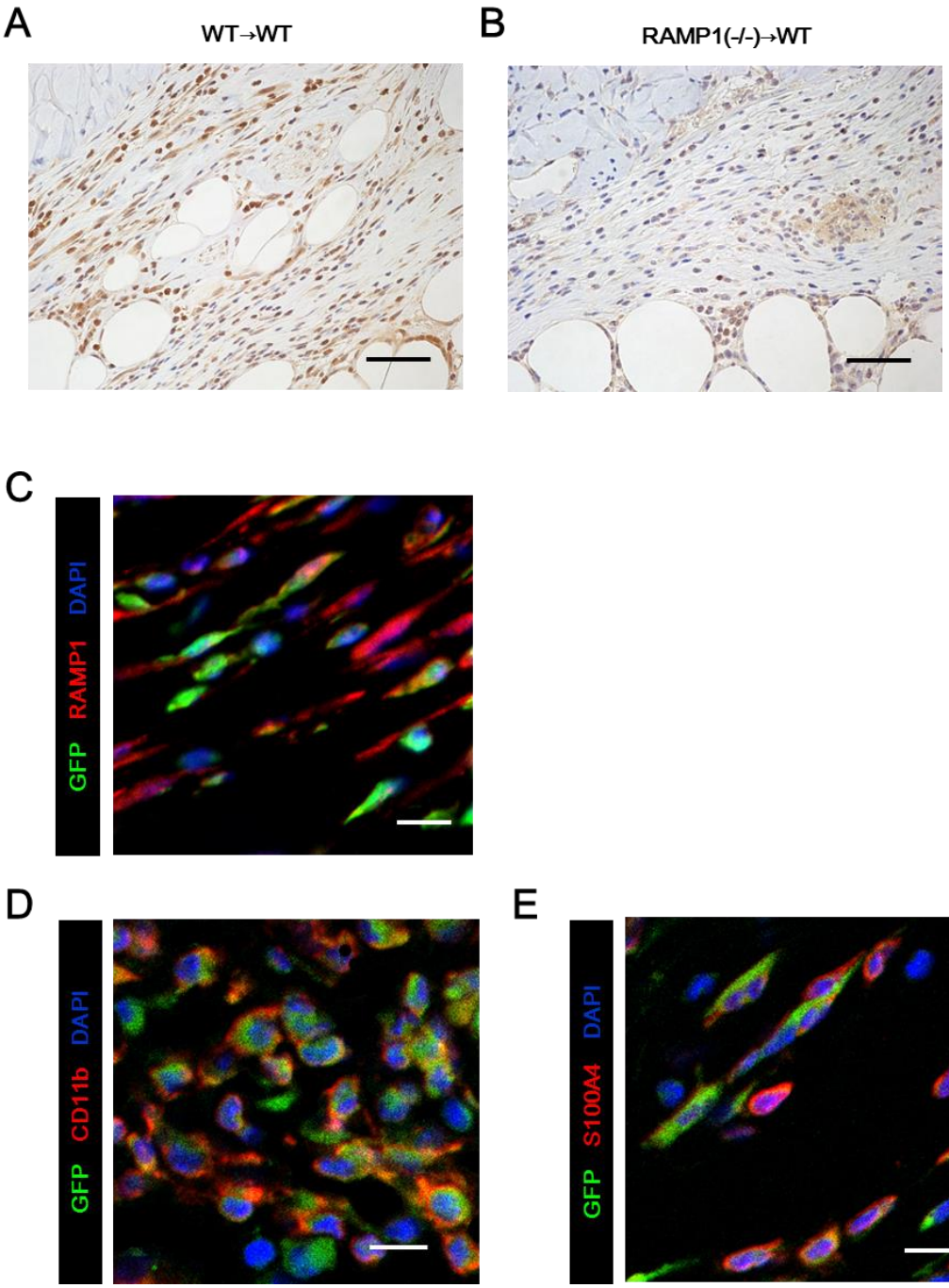
A
WT→WT
B
RAMP1(-/-)→WT
C
GFP RAMP1 DAPI
D
GFP CD11b DAPI
E
GFP S100A4 DAPI

Figure 8

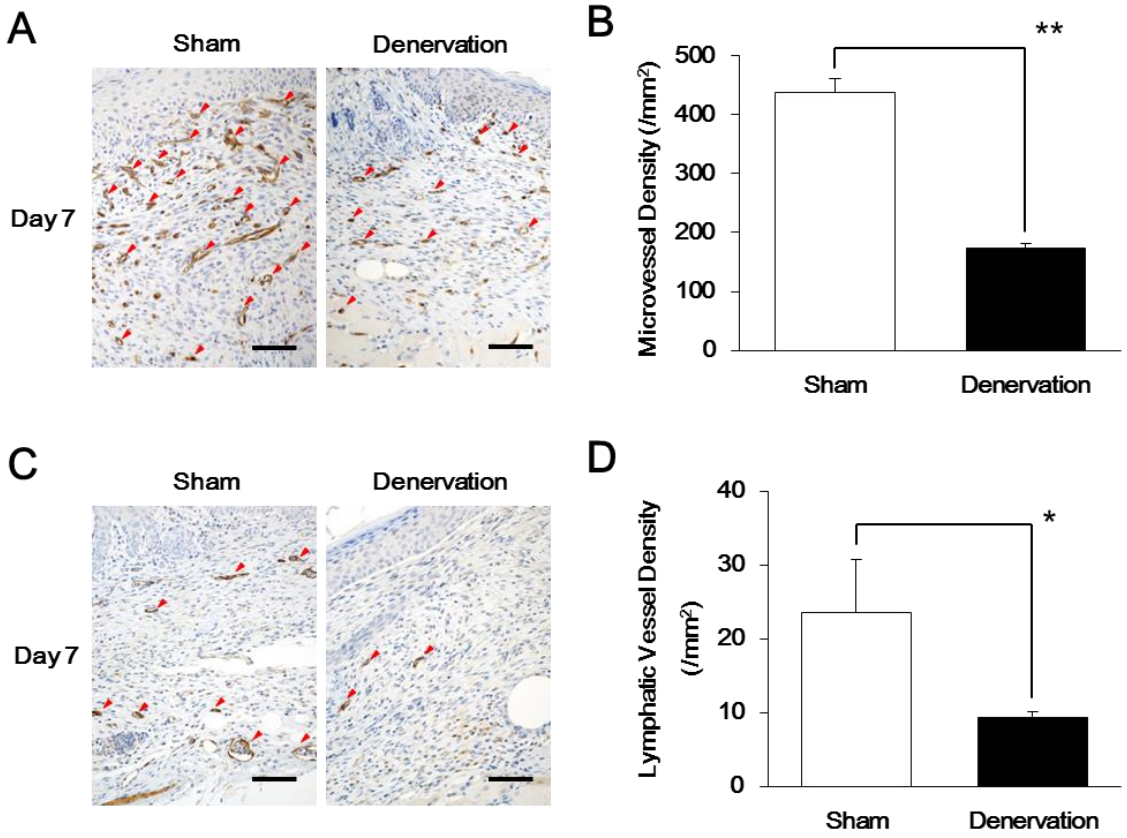

E

Day	Vehicle (%)	Capsaicin (%)
1	49.3 ± 2.7	77.7 ± 4.3**
4	30.8 ± 1.9	52.1 ± 2.4**
7	7.1 ± 1.0	11.7 ± 1.3**
10	1.9 ± 0.3	4.3 ± 0.5

Figure Legends

Figure 1. Reduced RAMP1 mRNA levels and delayed wound healing in RAMP1-/- mice

A-C) mRNA levels of pro-CGRP (A), CGRP (B), and RAMP1 (C) in DRGs. Data are expressed as means ± SEM of 4 mice/group. There was no difference between 2 groups before wounding (A, B), whereas a marked reduction in RAMP1 mRNA levels was seen in RAMP1-/- mice (C).

D) Time course of wound closure in RAMP1-/- and WT mice. Surgical wounds were made on the backs of RAMP1-/- mice and their WT counterparts, and wound closure was monitored as described in Materials and Methods. Data are expressed as means ± SEM of 8 mice/group. *$p < 0.05$, **$p < 0.01$ vs. WT mice.

E) Typical appearance of wounds in RAMP1-/- and WT mice at days 3, 5, and 7. Original diameter of the wounds was 6 mm.

Figure 2. Inhibition of wound-induced angiogenesis in RAMP1-/- mice

Surgical wounds were made on the backs of RAMP1-/- and their WT counterparts, and angiogenesis in the wound granulation tissues was monitored as described in Materials and Methods.

A) Double immunostaining of normal tissue in an uninjured lesion (left) and granulation tissue (right) from WT mice at day 5 with antibodies against CD31 (red) and RAMP1 (green). Scale bars = 100 μm.

B, C) Typical results of HE staining (day 6; B) and CD31 immunostaining (day 2-7; C) of wound granulation tissues in RAMP1-/- and WT mice. A reduced number of CD31-positive microvessels (brown stains indicated by red arrows) was observed in the granulation tissues of RAMP1-/- mice compared with that in WT mice. Scale bars = 100 μm.

D) Changes in microvessel density in granulation tissues at day 2-7. Tissues were stained for CD31 and photographed, and microvessels in the wound granulation tissues were counted. Microvessel density is expressed as microvessels per square millimeter. Data are expressed as means ± SEM from 6 mice/group; significantly different from WT mice at day 2-7. *$p < 0.05$ vs. WT mice.

E, F) mRNA expression levels of CD31 (E) and VEGF-A (F) in the wound granulation tissues of RAMP1-/- and WT mice determined by real-time RT-PCR at days 0, 2, 3, 5, 7, 10, and 14. Data are expressed as means ± SEM of 6 mice/group. *$p < 0.05$, **$p < 0.01$ vs. WT mice.

Figure 3. Effects of CGRP on the expression of VEGF-A, VEGF-C and VEGF-D in peritoneal thioglycolate-elicited macrophages and mouse fibroblast L929 cells

A) Double immunostaining of granulation tissue from WT mice at day 7 with antibodies against CD11b (red) and RAMP1 (green). Scale bar = 10 μm.

B) Double immunostaining of granulation tissue from WT mice at day 7 with antibodies against S100A4 (red) and RAMP1 (green). Scale bar = 20 μm.

C-E) Macrophages isolated from WT and RAMP1-/- mice were treated with CGRP agonists, and the mRNA levels of VEGF-A (C), VEGF-C (D), and VEGF-D (E) were determined 4 h after incubation. Real-time quantitative RT-PCR assays were used to assess mRNA expression. Data are expressed as means ± SEM of 3 independent experiments. *$p < 0.05$ vs. vehicle.

F-H) Mouse fibroblasts, L929 cells were treated with CGRP agonists for 4 h. mRNA levels of VEGF-A (F), VEGF-C (G), and VEGF-D (H) were determined by real-time quantitative RT-PCR assays. Data are expressed as means ± SEM of 3 independent experiments. CGRP agonists did not significantly increase VEGF-A, -C or -D production in L929 cells. *$p < 0.05$ vs. vehicle.

Figure 4. Inhibition of wound-induced lymphangiogenesis in RAMP1-/- mice

Surgical wounds were made on the backs of RAMP1-/- and their WT counterparts, and lymphangiogenesis in the wound granulation tissues was assessed, as described in Materials and Methods.

A) Double immunostaining of granulation tissues from WT mice at day 7 with antibodies against LYVE-1 (red) and RAMP1 (green). Scale bars = 50 μm.

B, C) Typical results of HE staining (day 7; B) and LYVE-1 immunostaining (day 3, 5, 6, 7, and 10; C) in the wound granulation tissues in RAMP1-/- and WT mice. A lesser number of LYVE-1-positive microvessels (brown stains indicated by red arrows) was observed in the granulation tissues of RAMP1-/- mice than in WT mice. Scale bars = 100 μm.

D) Changes in lymphatic vessel density in the granulation tissues at days 3, 5, 6, 7, and 10. Tissues were stained for LYVE-1 and photographed, and lymphatic vessels in the wound granulation tissues were counted. Lymphatic vessel density is expressed per square millimeter. Data are expressed as means ± SEM of 6 mice/group, significantly different from WT mice at days 6, 7, and 10. *$p < 0.05$ vs. WT mice.

E, F) mRNA expression levels of VEGF-C (E) and VEGFR-3 (F) in the wound granulation tissues of RAMP1-/- and WT mice, determined by real-time RT-PCR at days 0, 2, 3, 5, 7, 10, and 14. Data are expressed as means ± SEM of 6 mice/group. *$p < 0.05$, and **$p < 0.01$ vs. WT mice.

G) Fluorescence images of axillary lymph nodes 2 h after injection of 200 µl of 3% fluorescein isothiocyanate–dextran into the wounds on day 7 with a microsyringe. Scale bars = 5 mm. H) Quantification of the fluorescence of the extracted dye indicated that drainage from the wound area to the regional lymph nodes was reduced in RAMP1-/- mice (n = 5 for RAMP1-/-; n = 10 for WT).

Figure 5. Time course of wound healing, angiogenesis and lymphangiogenesis in mice with BM cells transplanted from RAMP1-/- mice

A lethal dose of radiation was administered to WT mice and BM cells from either WT mice or RAMP1-/- mice were injected into the tail vein (WT→WT or RAMP1-/-→WT). Surgical wounds were made on the backs of the mice, and wound closure was assessed as described in Materials and Methods.

A) Time course of wound closure in the WT mice transplanted with BM cells from RAMP1-/- or WT mice. Data are expressed as means ± SEM from 8 mice/group. *p < 0.05 and **p < 0.01 vs. WT mice.

B) Typical results of CD31 immunostaining of the wound granulation tissues in the WT mice with BM cells transplanted from RAMP1-/- or WT mice at day 3. A lesser number of CD31-positive microvessels (brown staining indicated by red arrows) was observed in the granulation tissues of RAMP1-/-→WT mice than in the WT→WT mice. Scale bars = 100 µm.

C) Microvessel density in granulation tissues on day 3. Data are expressed as means ± SEM from 6 mice/group, significantly different from WT→WT mice. **p < 0.01 vs. WT→WT mice.

D) Typical results of LYVE-1 immunostaining of the wound granulation tissues of WT mice with BM cells transplanted from either RAMP1-/- or WT mice at day 7. A lower number of LYVE-1-positive microvessels (brown staining indicated by red arrows) was observed in the granulation tissues of RAMP1-/-→WT mice than in WT→WT mice. Scale bars = 100 µm. E) Lymphatic vessel density in granulation tissues on day 7. Data are expressed as means ± SEM from 6 mice/group, significantly different from WT→WT mice. **p < 0.01 vs. WT→WT mice.

Figure 6. Temporal changes in the expressions of growth factors in wound granulation tissues

mRNA levels of EGF (A), TGFß (B), bFGF (C), and CTGF (D) in wound granulation tissues in RAMP1-/- and WT determined by real-time RT-PCR at day 0, 2, 3, 5, 7, 10, and 14. Data are expressed as the means ± SEM from four mice/group. *p < 0.05 vs. WT mice.

Figure 7. Representative immunohistochemical/immunofluorescence staining of RAMP1, CD11b and S100A4 in wound granulation tissues in BM chimera mice

A, B) A lethal dose of radiation was administered to WT mice and BM cells from either WT mice or RAMP1-/- mice were injected into the tail vein (A; WT→WT or B; RAMP1-/-→WT). Surgical wounds were made on the backs of the mice, and 7 days after wounding, wound granulation tissues were stained with antibodies against RAMP1 (brown). Counter stain was performed with Hematoxylin. Images are representative of three independent samples. Scale bar = 50 μm.

C, D, E) Seven days after wounding, wound granulation tissues in GFP BM chimera mice were stained with antibodies against RAMP1 (C; red), CD11b (D; red) or S1004A (E; red), and images were merged. Counter stain was performed with DAPI. Images are representative of three independent samples. Scale bar = 10 μm.

Figure 8. Effects of surgical denervation and chemical denervation on angiogenesis and lymphangiogenesis in wound granulation tissues

A) Typical results of CD31 immunostaining in wound granulation tissues made on the hind limbs in mice surgically denervated and in sham operated mice. Results from WT mice 7 days after wounding were shown. Reduced numbers of CD31-positive microvessels (brown stains indicated by red arrows) were observed in the granulation tissues in denervated WT mice. Scale bars = 100 μm.

B) Microvessel density in granulation tissues at day 7 in surgically denervated mice. Tissues were stained for CD31, and microvessel density in the wound granulation tissues was counted. Microvessel density was expressed as microvessels per mm^2. Data are expressed as means ± SEM from 6 mice/group; significantly different from WT mice at day 7 (**$p < 0.01$ vs. sham mice).

C) Typical results of LYVE-1 immunostaining in the wound granulation tissues made on the hind limbs in mice surgically denervated mice. Results from WT mice 7 days after wounding were shown. Reduced numbers of LYVE-1-positive microvessels (brown stains indicated by red arrows) were observed in the granulation tissues in denervated WT mice. Scale bars = 100 μm.

D) Lymphatic vessel density in granulation tissues at day 7 in surgically denervated mice. Tissues stained were for LYVE-1 and lymphatic vessels in the wound granulation tissues were counted. Density was expressed as microvessels per mm^2. Data are expressed as means ± SEM from 6 mice/ group; significantly different from sham operated mice at day 7 (*$p < 0.05$ vs. sham mice).

E) Effect of chemical denervation on wound healing. Healing process (% of original wound size) in capsaicin treated WT mice were compared with vehicle treated mice. Data are expressed as means ± SEM from sixteen mice/group; significantly different from vehicle treated mice at day 1, 4 and 7 (**$p < 0.01$ vs. vehicle treated mice).